Nonlinear optics in photonic nanowires

Mark A. Foster[1], **Amy C. Turner**[2], **Michal Lipson**[2], **and Alexander L. Gaeta**[1]

[1]*School of Applied and Engineering Physics, Cornell University, Ithaca, NY 14853*
[2]*School of Electrical and Computer Engineering, Cornell University, Ithaca, NY 14853*

alg3@cornell.edu

Abstract: We review recent research on nonlinear optical interactions in waveguides with sub-micron transverse dimensions, which are termed photonic nanowires. Such nanowaveguides, fabricated from glasses or semiconductors, provide the maximal confinement of light for index guiding structures enabling large enhancement of nonlinear interactions and group-velocity dispersion engineering. The combination of these two properties make photonic nanowires ideally suited for many nonlinear optical applications including the generation of single-cycle pulses and optical processing with sub-mW powers.

© 2008 Optical Society of America

OCIS codes: (190.4370) Nonlinear optics, fibers; (190.4390) Nonlinear optics, integrated optics

References and links

1. P. Dumais, F. Gonthier, S. Lacroix, A. Villeneuve, P. G. J. Wigley, and G. I. Stegeman, "Enhanced self-phase modulation in tapered fibers," Opt. Lett. **18**, 1996–1998 (1993).
2. D. Akimov, M. Schmitt, R. Maksimenka, K. Dukel'skii, Y. Kondrat'ev, A. Khokhlov, V. Shevandin, W. Kiefer, and A. M. Zheltikov, "Supercontinuum generation in a multiple-submicron-core microstructure fiber: toward limiting waveguide enhancement of nonlinear-optical processes," Appl. Phys. B **77**, 299–305 (2003).
3. A. M. Zheltikov, "The physical limit for the waveguide enhancement of nonlinear-optical processes," Opt. Spectrosc. **95**, 410–415 (2003).
4. V. Finazzi, T. M. Monro, and D. J. Richardson, "The role of confinement loss in highly nonlinear silica holey fibers," IEEE Photon. Technol. Lett. **15**, 1246–1248 (2003).
5. M. A. Foster, K. D. Moll, A. L. Gaeta, "Optimal waveguide dimensions for nonlinear interactions," Opt. Express **12**, 2880–2887 (2004), http://www.opticsexpress.org/abstract.cfm?URI=OPEX-12-13-2880.
6. Y. Lize, E. Magi, V. Ta'eed, J. Bolger, P. Steinvurzel, and B. Eggleton, "Microstructured optical fiber photonic wires with subwavelength core diameter," Opt. Express **12**, 3209–3217 (2004), http://www.opticsinfobase.org/abstract.cfm?URI=oe-12-14-3209.
7. C. Koos, L. Jacome, C. Poulton, J. Leuthold, and W. Freude, "Nonlinear silicon-on-insulator waveguides for all-optical signal processing," Opt. Express **15**, 5976–5990 (2007), http://www.opticsinfobase.org/abstract.cfm?URI=oe-15-10-5976.
8. L. M. Tong, R. R. Gattass, J. B. Ashcom, S. L. He, J. Y. Lou, M. Y. Shen, I. Maxwell, and E. Mazur, "Subwavelength-diameter silica wires for low-loss optical wave guiding," Nature **426**, 816–819 (2003).
9. M. Hu, C. -y. Wang, Y. Li, Z. Wang, L. Chai, and A. Zheltikov, "Multiplex frequency conversion of unamplified 30-fs Ti: sapphire laser pulses by an array of waveguiding wires in a random-hole microstructure fiber," Opt. Express **12**, 6129–6134 (2004), http://www.opticsinfobase.org/abstract.cfm?URI=oe-12-25-6129
10. S. Leon-Saval, T. Birks, W. Wadsworth, P. St. J. Russell, M. Mason, "Supercontinuum generation in submicron fibre waveguides," Opt. Express **12**, 2864–2869 (2004), http://www.opticsexpress.org/abstract.cfm?URI=OPEX-12-13-2864.
11. N. A. Wolchover, F. Luan, A. K. George, J. C. Knight, and F. G. Omenetto, "High nonlinearity glass photonic crystal nanowires," Opt. Express **15**, 829–833 (2007), http://www.opticsinfobase.org/abstract.cfm?URI=oe-15-3-829.
12. C. Grillet, C. Smith, D. Freeman, S. Madden, B. Luther-Davies, E. Magi, D. Moss, and B. Eggleton, "Efficient coupling to chalcogenide glass photonic crystal waveguides via silica optical fiber nanowires," Opt. Express **14**, 1070–1078 (2006), http://www.opticsinfobase.org/abstract.cfm?URI=oe-14-3-1070.

#89450 - $15.00 USD Received 6 Nov 2007; revised 5 Jan 2008; accepted 5 Jan 2008; published 16 Jan 2008

13. J. S. Foresi, P. R. Villeneuve, J. Ferrera, E. R. Thoen, G. Steinmeyer, S. Fan, J. D. Joannopoulos, L. C. Kimerling, H. I. Smith, and E. P. Ippen, "Photonic-bandgap microcavities in optical waveguides," Nature **390**, 143–145 (1997).
14. Y. A. Vlasov and S. J. McNab, "Losses in single-mode silicon-on-insulator strip waveguides and bends," Opt. Express **12**, 1622–1631 (2004), http://www.opticsinfobase.org/abstract.cfm?URI=oe-12-8-1622.
15. J. P. Zhang, D. Y. Chu, S. L. Wu, S. T. Ho, W. G. Bi, C. W. Tu, R. C. Tiberio, "Photonic-wire laser," Phys. Rev. Lett. **75**, 2678–2681 (1995).
16. G. A. Siviloglou, S. Suntsov, R. El-Ganainy, R. Iwanow, G. I. Stegeman, D. N. Christodoulides, R. Morandotti, D. Modotto, A. Locatelli, C. De Angelis, F. Pozzi, C. R. Stanley, and M. Sorel, "Enhanced third-order nonlinear effects in optical AlGaAs nanowires," Opt. Express **14**, 9377–9384 (2006), http://www.opticsinfobase.org/abstract.cfm?URI=oe-14-20-9377.
17. L. Tong, J. Lou, and E. Mazur, "Single-mode guiding properties of subwavelength-diameter silica and silicon wire waveguides," Opt. Express **12**, 1025–1035 (2004), http://www.opticsinfobase.org/abstract.cfm?URI=oe-12-6-1025.
18. L. Yin, Q. Lin, G. P. Agrawal, "Dispersion tailoring and soliton propagation in silicon waveguides," Opt. Lett. **31**, 1295–1297 (2006).
19. E. Dulkeith, F. Xia, L. Schares, W. M. J. Green, Y. A. Vlasov, "Group index and group velocity dispersion in silicon-on-insulator photonic wires," Opt. Express. **14**, 3853–3863 (2006), http://www.opticsinfobase.org/abstract.cfm?URI=oe-14-9-3853 .
20. A. C. Turner, C. Manolatou, B. S. Schmidt, M. Lipson, M. A. Foster, J. E. Sharping, A. L. Gaeta, "Tailored anomalous group-velocity dispersion in silicon channel waveguides," Opt. Express **14**, 4357–4362 (2006), http://www.opticsinfobase.org/abstract.cfm?URI=oe-14-10-4357.
21. V. R. Almeida, C. A. Barrios, R. R. Panepucci, M. Lipson, M. A. Foster, D. G. Ouzounov, and A. L. Gaeta, "All-optical switching on a silicon chip," Opt. Lett. **29**, 2867–2869 (2004).
22. R. Espinola, J. Dadap, R. Osgood, Jr., S. McNab, and Y. Vlasov, "Raman amplification in ultrasmall silicon-on-insulator wire waveguides," Opt. Express **12**, 3713–3718 (2004), http://www.opticsinfobase.org/abstract.cfm?URI=oe-12-16-3713.
23. D. Dimitropoulos, R. Jhaveri, R. Claps, J. C. S. Woo, and B. Jalali, "Lifetime of photogenerated carriers in silicon-on-insulator rib wavegudies," Appl. Phys. Lett. **86** 071115 (2005).
24. A. Zheltikov, "Gaussian-mode analysis of waveguide-enhanced Kerr-type nonlinearity of optical fibers and photonic wires," J. Opt. Soc. Am. B **22** 1100–1104 (2005).
25. G. P. Agrawal, *Nonlinear Fiber Optics* (Academic Press, Boston, 1989).
26. A. W. Snyder and J. D. Love, *Optical Waveguide Theory* (Kluwer Academic Publishers, 1983).
27. C. R. Pollock and M. Lipson, *Integrated Photonics* (Kluwer Academic Publishers, 2003).
28. J. K. Ranka, R. S. Windeler, and A. J. Stentz, "Visible continuum generation in air silica microstructure optical fibers with anomalous dispersion at 800nm," Opt. Lett. **25**, 25–27 (2000).
29. W. J. Wadsworth, A. Ortigosa-Blanch, J. C. Knight, T. A. Birks, T. -P. M. Man, and P. S. J. Russell, "Supercontinuum generation in photonic crystal fibers and optical fiber tapers: a novel light source," J. Opt. Soc. Am. B **19**, 2148–2155 (2002).
30. A. V. Husakou and J. Herrmann, "Supercontinuum generation of higher-order solitons by fission in photonic crystal fibers," Phys. Rev. Lett. **87**, 203901 (2001).
31. A. L. Gaeta, "Nonlinear propagation and continuum generation in microstructured optical fibers," Opt. Lett. **27**, 924–926 (2002).
32. J. M. Dudley and S. Coen, "Numerical simulations and coherence properties of supercontinuum generation in photonic crystal and tapered optical fibers," IEEE J. Sel. Top. Quantum Electron. **8**, 651–659 (2002).
33. J. M. Dudley, L. Provino, N. Grossard, H. Maillotte, R. S. Windeler, B. J. Eggleton, and S. Coen, "Supercontinuum generation in air-silica microstrcutured fibers with nanosecond and femtosecond pulse pumping," J. Opt. Soc. Am. B **19**, 765–771 (2002).
34. J. M. Dudley, G. Genty, and S. Coen, "Supercontinuum generation in photonic crystal fiber," Rev. Mod. Phys. **78**, 1135–1184 (2006).
35. T. A. Birks and Y. W. Li, "The shape of fiber tapers," J. Lightwave Technol. **10**, 432–438 (1992).
36. L. Shi, X. Chen, H. Liu, Y. Chen, Z. Ye, W. Liao, and Y. Xia, "Fabrication of submicron-diameter silica fibers using electric strip heater," Opt. Express **14**, 5055–5060 (2006), http://www.opticsinfobase.org/abstract.cfm?URI=oe-14-12-5055.
37. R. R. Gattass, G. T. Svacha, L. Tong, and E. Mazur, "Supercontinuum generation in submicrometer diameter silica fibers," Opt. Express **14**, 9408–9414 (2006), http://www.opticsinfobase.org/abstract.cfm?URI=oe-14-20-9408.
38. E. Magi, P. Steinvurzel, and B. Eggleton, "Tapered photonic crystal fibers," Opt. Express **12**, 776–784 (2004), http://www.opticsinfobase.org/abstract.cfm?URI=oe-12-5-776.
39. M. A. Foster and A. L. Gaeta, "Ultra-low threshold supercontinuum generation in sub-wavelength waveguides," Opt. Express **12**, 3137–3143 (2004), http://www.opticsinfobase.org/abstract.cfm?URI=oe-12-14-3137.
40. L. Tong, L. Hu, J. Zhang, J. Qiu, Q. Yang, J. Lou, Y. Shen, J. He, and Z. Ye, "Pho-

#89450 - $15.00 USD Received 6 Nov 2007; revised 5 Jan 2008; accepted 5 Jan 2008; published 16 Jan 2008
(C) 2008 OSA

tonic nanowires directly drawn from bulk glasses," Opt. Express **14**, 82–87 (2006), http://www.opticsinfobase.org/abstract.cfm?URI=oe-14-1-82.
41. E. Magi, H. Nguyen, and B. Eggleton, "Air-hole collapse and mode transitions in microstructured fiber photonic wires," Opt. Express **13**, 453–459 (2005), http://www.opticsinfobase.org/abstract.cfm?URI=oe-13-2-453.
42. M. Kolesik and J. V. Moloney, "Nonlinear optical pulse propagation simulation: From Maxwell's to unidirectional equations," Phys. Rev. E **70**, 036604 (2004).
43. M. Kolesik, E. M. Wright, and J. V. Moloney, "Simulation of femtosecond pulse propagation in sub-micron diameter tapered fibers," Appl. Phys. B **79**, 293–300 (2004).
44. B. Kibler, J. M. Dudley, and S. Coen, "Supercontinuum generation and nonlinear pulse propagation in photonic crystal fiber: influence of the frequency-dependent effective area," Appl. Phys. B **81**, 337–342 (2005).
45. M. A. Foster, J. M. Dudley, B. Kibler, Q. Cao, D. Lee, R. Trebino, and A. L. Gaeta, "Nonlinear pulse propagation and supercontinuum generation in photonic nanowires: experiment and simulation," Appl. Phys. B **81**, 363–367 (2005).
46. B. T. Kuhlmey, H. C. Nguyen, M. J. Steel, and B. J. Eggleton, "Confinement loss in adiabatic photonic crystal fiber tapers," J. Opt. Soc. Am. B **23**, 1965–1974 (2006).
47. C. M. B. Cordeiro, W. J. Wadsworth, T. A. Birks, and P. S. J. Russell, "Engineering the dispersion of tapered fibers for supercontinuum generation with a 1064 nm pump laser," Opt. Lett. **30**, 1980–1982 (2005).
48. J. C. Travers, S. V. Popov, and J. R. Taylor, "Extended blue supercontinuum generation in cascaded holey fibers," Opt. Lett. **30**, 3132–3134 (2005).
49. C. Xiong, A. Witkowska, S. G. Leon-Saval, T. A. Birks, and W. J. Wadsworth, "Enhanced visible continuum generation from a microchip 1064nm laser," Opt. Express **14**, 6188–6193 (2006), http://www.opticsinfobase.org/abstract.cfm?URI=oe-14-13-6188.
50. M. A. Foster, A. L. Gaeta, Q. Cao, and R. Trebino, "Soliton-effect compression of supercontinuum to few-cycle durations in photonic nanowires," Opt. Express **13**, 6848–6855 (2005), http://www.opticsinfobase.org/abstract.cfm?URI=oe-13-18-6848.
51. M. A. Foster, Q. Cao, R. Trebino, and A. L. Gaeta, "Pulse Self-Compression of Supercontinuum in Photonic Nanowires," in 15th International Conference on Ultrafast Phenomena, OSA Technical Digest Series (CD) (Optical Society of America, 2006), paper WC5.
52. M. V. Tognetti and H. M. Crespo, "Sub-two-cycle soliton-effect pulse compression at 800 nm in photonic crystal fibers," J. Opt. Soc. Am. B **24**, 1410–1415 (2007).
53. N. Akhmediev and M. Karlsson, "Cherenkov radiation emitted by solitons in optical fibers," Phys. Rev. A **51**, 2602–2607 (1995).
54. I. Cristiani, R. Tediosi, L. Tartara, and V. Degiorgio, "Dispersive wave generation by solitons in microstructured optical fibers," Opt. Express **12**, 124–135 (2004), http://www.opticsinfobase.org/abstract.cfm?URI=oe-12-1-124.
55. A. B. Fedotov, S. O. Konorov, E. E. Serebryannikov, D. A. Sidorov-Biryukov, V. P. Mitrokhin, K, V, Dukel'skii, A. V. Khokhlov, V. S. Shevandin, Yu. N. Kondrat'ev, M. Scalora, and A. M. Zheltikov, "Assorted non-linear optics in microchannel waveguides of photonic-crystal fibers," Opt. Commun. **255**, 218–224 (2005).
56. S. O. Konorov, D. A. Akimov, E. E. Serebryannikov, A. A. Ivanov, M. V. Alfimov, K. V. Dukel'skii, A. V. Khokhlov, V. S. Shevandin, Yu. N. Kondrat'ev, and A. M. Zheltikov, "High-order modes of photonic wires excited by the Cherenkov emission of solitons," Laser Phys. Lett. **2**, 258–261 (2005).
57. D. Akimov, T. Siebert, W. Kiefer, and A. Zheltikov, "Optical parametric amplification of a blueshifted output of a photonic-crystal fiber," J. Opt. Soc. Am. B **23**, 1988–1993 (2006).
58. H. K. Tsang, C. S. Wong, T. K. Liang, I. E. Day, S. W. Roberts, A. Harpin, J. Drake, M. Asghari, "Optical dispersion, two-photon absorption and self-phase modulation in silicon waveguides at 1.5 m wavelength," Appl. Phys. Lett. **80**, 416–418 (2002).
59. M. Dinu, F. Quochi, H. Garcia, "Third-order nonlinearities in silicon at telecom waveguides," Appl. Phys. Lett. **82**, 2954–2956 (2003).
60. D. J. Moss, L. Fu, I. Littler, B. J. Eggleton, "Ultrafast all-optical modulation via two-photon absorption in silicon-on-insulator waveguides," Electron. Lett. **41**, 320–321 (2005).
61. T. Liang, L. Nunes, T. Sakamoto, K. Sasagawa, T. Kawanishi, M. Tsuchiya, G. Priem, D. Van Thourhout, P. Dumon, R. Baets, H. Tsang, "Ultrafast all-optical switching by cross-absorption modulation in silicon wire waveguides," Opt. Express **13**, 7298–7303 (2005), http://www.opticsinfobase.org/abstract.cfm?URI=oe-13-19-7298.
62. T. K. Liang, L. R. Nunes, M. Tsuchiya, K. S. Abedin, T. Miyazaki, D. Van Thourhout, W. Bogaerts, P. Dumon, R. Baets, H. K. Tsang, "High speed logic gate using two-photon absoprtion in silicon waveguides," Opt. Commun. **265** 171–174 (2006).
63. R. A. Soref, B. R. Bennett, "Electrooptical effects in silicon," IEEE J. Quantum Electron. **23**, 123–129 (1987).
64. S. Stepanov, S. Ruschin, "Modulation of light by light in silicon-on-insulator waveguides," Appl. Phys. Lett. **83**, 5151–5153 (2003).
65. V. R. Almeida, C. A. Barrios, R. R. Panepucci, M. Lipson, "All-optical control of light on a silicon chip," Nature **431**, 1081–1084 (2004).
66. V. R. Almeida, Q. Xu, M. Lipson, "Ultrafast integrated semiconductor optical modulator based on the plasma-

#89450 - $15.00 USD Received 6 Nov 2007; revised 5 Jan 2008; accepted 5 Jan 2008; published 16 Jan 2008
(C) 2008 OSA

dispersion effect," Opt. Lett. **30** 2403–2405 (2005).
67. S. F. Preble, Q. Xu, B. S. Schmidt, M. Lipson, "Ultrafast all-optical modulation on a silicon chip," Opt. Lett. **30** 2891–2893 (2005).
68. Q. Xu, M. Lipson, "Carrier-induced optical bistability in silicon ring resonators," Opt. Lett. **31** 341–343 (2006).
69. C. Manolatou, M. Lipson, "All-optical silicon modulators based on carrier injection by two-photon absorption," J. Lightwave Technol. **24** 1433–1439 (2006).
70. Q. Xu, M. Lipson, "All-optical logic based on silicon micro-ring resonators," Opt. Express **15** 924–929 (2007), http://www.opticsinfobase.org/abstract.cfm?URI=oe-15-3-924.
71. S. F. Preble, Q. Xu, M. Lipson, "Changing the colour of light in a silicon resonator," Nature Photonics **1** 293–296 (2007).
72. P. Dong, S. F. Preble, M. Lipson, "All-optical compact silicon comb switch," Opt. Express **15** 9600–9605 (2007), http://www.opticsinfobase.org/abstract.cfm?URI=oe-15-15-9600.
73. R. Claps, D. Dimitropoulos, Y. Han, B. Jalali, "Observation of Raman emission in silicon waveguides at 1.54 m," Opt. Express **10**, 1305–1313 (2002), http://www.opticsexpress.org/abstract.cfm?URI=OPEX-10-22-1305.
74. R. Claps, D. Dimitropoulos, B. Jalali, "Stimulated Raman scattering in silicon waveguides," IEEE Electron. Lett. **38**, 1352–1354 (2002).
75. R. Claps, D. Dimitropoulos, V. Raghunathan, Y. Han, B. Jalali, "Observation of stimulated Raman amplification in silicon waveguides," Opt. Express **11**, 1731–1739 (2003), http://www.opticsinfobase.org/abstract.cfm?URI=oe-11-15-1731.
76. T. K. Liang, H. K. Tsang, "Role of free carriers from two-photon absorption in Raman amplification in silicon-on-insulator waveguides," Appl. Phys. Lett. **84**, 2745–2747 (2004).
77. R. Claps, V. Raghunathan, D. Dimitropoulos, B. Jalali, "Influence of nonlinear absorption on Raman amplification in Silicon waveguides," Opt. Express **12**, 2774–2780 (2004), http://www.opticsexpress.org/abstract.cfm?URI=OPEX-12-12-2774.
78. Q. Xu, V. Almeida, M. Lipson, "Time-resolved study of Raman gain in highly confined silicon-on-insulator waveguides," Opt. Express **12**, 4437–4442 (2004), http://www.opticsinfobase.org/abstract.cfm?URI=oe-12-19-4437.
79. O. Boyraz, B. Jalali, "Demonstration of a silicon Raman laser," Opt. Express **12**, 5269–5273 (2004), http://www.opticsinfobase.org/abstract.cfm?URI=oe-12-21-5269.
80. J. I. Dadap, R. L. Espinola, R. M. Osgood Jr., S. J. McNab, Y. A. Vlasov, "Spontaneous Raman scattering in ultrasmall silicon waveguides," Opt. Lett. **29**, 2755–2757 (2004).
81. Q. Xu, V. R. Almeida, M. Lipson, "Demonstration of high Raman gain in a submicrometer-size silicon-on-insulator waveguide," Opt. Lett. **30**, 35–37 (2005).
82. V. Raghunathan, R. Claps, D. Dimitropoulos, B. Jalali, "Parametric Raman Wavelength Conversion in Scaled Silicon Waveguides," J. Lightwave Technol. **23**, 2094–2102 (2005).
83. R. Jones, H. Rong, A. Liu, A. Fang, M. Paniccia, D. Hak, O. Cohen, "Net continuous wave optical gain in a low loss silicon-on-insulator waveguide by stimulated Raman scattering," Opt. Express **13**, 519–525 (2005), http://www.opticsinfobase.org/abstract.cfm?URI=oe-13-2-519.
84. H. Rong, A. Liu, R. Jones, O. Cohen, D. Hak, R. Nicolaescu, A. Fang, M. Panniccia, "An all-silicon Raman laser," Nature **433**, 292–294 (2005).
85. H. Rong, R. Jones, A. Liu, O. Cohen, D. Hak, A. Fang, M. Paniccia, "A continuous-wave Raman silicon laser," Nature **433**, 725–728 (2005).
86. S. Blair, K. Zheng, "Intensity-tunable group delay using stimulated Raman scattering in silicon slow-light waveguides," Opt. Express **14**, 1064–1069 (2006), http://www.opticsinfobase.org/abstract.cfm?URI=oe-14-3-1064.
87. Y. Okawachi, M. A. Foster, J. E. Sharping, A. L. Gaeta, Q. Xu, M. Lipson, "All-optical slow-light on a photonic chip," Opt. Express **14**, 2317–2322 (2006), http://www.opticsinfobase.org/abstract.cfm?URI=oe-14-6-2317.
88. D. Dimitropoulos, V. Raghunathan, R. Claps, B. Jalali, "Phase-matching and nonlinear optical processes in silicon waveguides," Opt. Express **12**, 149–160 (2004), http://www.opticsinfobase.org/abstract.cfm?URI=oe-12-1-149.
89. O. Boyraz, T. Indukuri, B. Jalali, "Self-phase-modulation induced spectral broadening in silicon waveguides," Opt. Express **12**, 829–834 (2004), http://www.opticsinfobase.org/abstract.cfm?URI=oe-12-5-829.
90. A. Cowan, G. Rieger, J. Young, "Nonlinear transmission of 1.5 m pulses through single-mode silicon-on-insulator waveguide structures," Opt. Express **12**, 1611–1621 (2004), http://www.opticsinfobase.org/abstract.cfm?URI=oe-12-8-1611.
91. O. Boyraz, P. Koonath, V. Raghunathan, B. Jalali, "All optical switching and continuum generation in silicon waveguides," Opt. Express **12**, 4094–4102 (2004), http://www.opticsinfobase.org/abstract.cfm?URI=oe-12-17-4094.
92. R. L. Espinola, J. I. Dadap, R. M. Osgood, S. J. McNab, Y. A. Vlasov, "C-band wavelength conversion in silicon photonic wire waveguides," Opt. Express **13**, 4341–4349 (2005), http://www.opticsinfobase.org/abstract.cfm?URI=oe-13-11-4341.
93. H. Fukuda, K. Yamada, T. Shoji, M. Takahashi, T. Tsuchizawa, T. Watanabe, J. Takahashi, S.

#89450 - $15.00 USD Received 6 Nov 2007; revised 5 Jan 2008; accepted 5 Jan 2008; published 16 Jan 2008
(C) 2008 OSA

Itabashi, "Four-wave mixing in silicon wire waveguides," Opt. Express **13**, 4629–4637 (2005), http://www.opticsinfobase.org/abstract.cfm?URI=oe-13-12-4629.
94. H. Rong, Y. -H. Kuo, A. Liu, M. Paniccia, O. Cohen, "High efficiency wavelength conversion of 10 Gb/s data in silicon waveguides," Opt. Express **14**, 1182–1188 (2006), http://www.opticsinfobase.org/abstract.cfm?URI=oe-14-3-1182.
95. M. A. Foster, A. C. Turner, J. E. Sharping, B. S. Schmidt, M. Lipson, A. L. Gaeta, "Broad-band optical parametric gain on a silicon photonic chip," Nature **441**, 960–963 (2006).
96. K. Yamada, H. Fukuda, T. Tsuchizawa, T. Watanabe, T. Shoji, S. Itabashi, "All-optical efficient wavelength conversion using silicon photonic wire waveguide," IEEE Photon. Technol. Lett. **18**, 1046–1048 (2006).
97. Q. Lin, J. Zhang, P. M. Fauchet, G. P. Agrawal, "Ultrabroadband parametric generation and wavelength conversion in silicon waveguides," Opt. Express **14**, 4786–4799 (2006), http://www.opticsinfobase.org/abstract.cfm?URI=oe-14-11-4786.
98. E. Dulkeith, Y. A. Vlasov, X. Chen, N. C. Panoiu, R. M. Osgood, Jr., "Self-phase-modulation in submicron silicon-on-insulator photonic wires," Opt. Express **14**, 5524–5534 (2006), http://www.opticsinfobase.org/abstract.cfm?URI=oe-14-12-5524.
99. R. Dekker, A. Driessen, T. Wahlbrink, C. Moormann, J. Niehusmann, M. Forst, "Ultrafast Kerr-induced all-optical wavelength conversion in silicon waveguides using 1.55 m femtosecond pulses," Opt. Express **14**, 8336–8346 (2006), http://www.opticsinfobase.org/abstract.cfm?URI=oe-14-18-8336.
100. Y. -H. Kuo, H. Rong, V. Sih, S. Xu, M. Paniccia, O. Cohen, "Demonstration of wavelength conversion at 40 Gb/s data rate in silicon waveguides," Opt. Express **14**, 11721–11726 (2006), http://www.opticsinfobase.org/abstract.cfm?URI=oe-14-24-11721.
101. I. W. Hsieh, X. Chen, J. I. Dadap, N. C. Panoiu, R. M. Osgood, S. J. McNab, Y. A. Vlasov, "Ultrafast-pulse self-phase modulation and third-order dispersion in Si photonic wire-waveguides," Opt. Express **14**, 12380–12387 (2006), http://www.opticsinfobase.org/abstract.cfm?URI=oe-14-25-12380.
102. J. E. Sharping, K. F. Lee, M. A. Foster, A. C. Turner, B. S. Schmidt, M. Lipson, A. L. Gaeta, P. Kumar, "Generation of correlated photons in nanoscale silicon waveguides," Opt. Express **14**, 12388–12393 (2006), http://www.opticsinfobase.org/abstract.cfm?URI=oe-14-25-12388.
103. L. Yin, Q. Lin, G. P. Agrawal, "Soliton fission and supercontinuum generation in silicon waveguides," Opt. Lett. **32**, 391–393 (2007).
104. I. W. Hsieh, X. Chen, J. I. Dadap, N. C. Panoiu, R. M. Osgood, Jr., S. J. McNab, Y. A. Vlasov, "Cross-phase modulation-induced spectral and temporal effects on co-propagating femtosecond pulses in silicon photonic wires," Opt. Express **15**, 1135–1146 (2007), http://www.opticsinfobase.org/abstract.cfm?URI=oe-15-3-1135.
105. J. Zhang, Q. Lin, G. Piredda, R. W. Boyd, G. P. Agrawal, P. M. Fauchet, "Optical solitons in a silicon waveguide," Opt. Express **15**, 7682–7688 (2007), http://www.opticsinfobase.org/abstract.cfm?URI=oe-15-12-7682.
106. R. Salem, M. A. Foster, A. C. Turner, D. F. Geraghty, M. Lipson, A. L. Gaeta, "All-optical regeneration on a silicon chip," Opt. Express **15**, 7802–7809 (2007), http://www.opticsinfobase.org/abstract.cfm?URI=oe-15-12-7802.
107. M. A. Foster, A. C. Turner, R. Salem, M. Lipson, A. L. Gaeta, "Broad-band continuous-wave parametric wavelength conversion in silicon nanowaveguides," Opt. Express **15**, 12949–12958 (2007), http://www.opticsinfobase.org/abstract.cfm?URI=oe-15-20-12949.
108. R. Salem, M. A. Foster, A. C. Turner, D. F. Geraghty, M. Lipson, A. L. Gaeta, "Signal regeneration using low-power four-wave mixing on silicon chip," Nature Photonics **2**, 35–38 (2008).
109. A. C. Turner, M. A. Foster, A. L. Gaeta, and M. Lipson, "Ultra-low power nonlinear frequency conversion in a silicon photonic structure," submitted for publication.
110. I. W. Hsieh, X. G. Chen, X. P. Liu, J. I. Dadap, N. C. Panoiu, C. Y. Chou, F. N. Xia, W. M. Green, Y. A. Vlasov, and R. M. Osgood, "Supercontinuum generation in silicon photonic wires," Opt. Express **15**, 15242–15249 (2007).
111. A. D. Bristow, N, Rotenberg, H. M. van Driel, "Two-photon absorption and Kerr coefficiecnts of silicon for 850-2200 nm," Appl. Phys. Lett. **90**, 191104 (2007).
112. Q. Lin, J. Zhang, G. Piredda, R. W. Boyd, P. M. Fauchet, G. P. Agrawal, "Dispersion of silicon nonlinearities in the near infrared region," Appl. Phys. Lett. **91**, 021111 (2007).
113. A. Chin, K. Y. Lee, B. C. Lin, S. Horng, "Picosecond photoresponse of carriers in Si ion-implanted Si," Appl. Phys. Lett. **69**, 653–655 (1996).
114. P. V. Mamyshev, "All-optical data regeneration based on self-phase modulation effect," in Proc. European Conference on Optical Communications (ECOC98), p. 475, (1998).
115. K. P. Nayak, P. N. Melentiev, M. Morinaga, F. L. Kien, V. I. Balykin, K. Hakuta, "Optical nanofiber as an efficient tool for manipulating and probing atomic fluorescence," Opt. Express **15**, 5431–5438 (2007), http://www.opticsinfobase.org/abstract.cfm?URI=oe-15-9-5431.
116. E. C. Magi, L. B. Fu, H. C. Nguyen, M. R. Lamont, D. I. Yeom, B. J. Eggleton, "Enhanced Kerr nonlinearity in sub-wavelength diameter As_2Se_3 chalcogenide fiber tapers," Opt. Express **15**, 10324–10329 (2007), http://www.opticsinfobase.org/abstract.cfm?URI=oe-15-16-10324.
117. M. R. Lamont, C. M. de Sterke, and B. J. Eggleton, "Dispersion engineering of highly nonlinear As_2S_3 waveguides for parametric gain and wavelength conversion," Opt. Express **15**, 9458–9463 (2007),

#89450 - $15.00 USD Received 6 Nov 2007; revised 5 Jan 2008; accepted 5 Jan 2008; published 16 Jan 2008
(C) 2008 OSA

http://www.opticsinfobase.org/abstract.cfm?URI=oe-15-15-9458.
118. P. P. Absil, J. V. Hryniewicz, B. E. Little, P. S. Cho, R. A. Wilson, L. G. Joneckis, P. T. Ho, "Wavelength conversion in GaAs micro-ring resonators," Opt. Lett. **25**, 554–556 (2000).
119. V. Van, T. A. Ibrahim, P. P. Absil, F. G. Johnson, R. Grover, P. T. Ho, "Optical signal processing using nonlinear semiconductor microring resonators," IEEE J. Sel. Tops. Quantum Electron. **8**, 705–713 (2002).
120. J. E. Heebner, N. N. Lepeshkin, A. Schweinsberg, G. W. Wicks, R. W. Boyd, R. Grover, P. T. Ho, "Enhanced linear and nonlinear optical phase response of AlGaAs microring resonators," Opt. Lett. **29**, 769–771 (2004).
121. R. El-Ganainy, S. Mokhov, K. G. Makris, D. N. Christodoulides, R. Morandotti, "Solitons in dispersion-inverted AlGaAs nanowires," Opt. Express **14**, 2277–2282 (2006), http://www.opticsinfobase.org/abstract.cfm?URI=oe-14-6-2277.
122. J. Meier, W. S. Mohammed, A. Jugessur, L. Qian, M. Mojahedi, J. S. Aitchison, "Group velocity inversion in AlGaAs nanowires," Opt. Express **15**, 12755–12762 (2007), http://www.opticsinfobase.org/abstract.cfm?URI=oe-15-20-12755.
123. F. Benabid, J. C. Knight, G. Antonopoulos, and P. St. J. Russell, "Stimulated Raman scattering in hydrogen-filled hollow-core photonic crystal fiber," Science **298**, 399–402 (2002).
124. D. G. Ouzounov, F. R. Ahmad, D. Muller, N. Venkataraman, M. T. Gallagher, M. G. Thomas, J. Silcox, K. W. Koch, and A. L. Gaeta, "Generation of megawatt optical solitons in hollow-core photonic band-gap fibers," Science **301**, 1702–1704 (2003).
125. F. Benabid, G. Bouwmans, J. C. Knight, and P. St. J. Russell, "Ultrahigh efficiency laser wavelength conversion in a gas-filled hollow core photonic crystal fiber by pure stimulated Raman scattering in molecular hydrogen," Phys. Rev. Lett. **93**, 123903 (2004).
126. S. Ghosh, J. E. Sharping, D. G. Ouzounov, and A. L. Gaeta, "Resonant optical interactions with molecules confined in photonic band-gap fibers," Phys. Rev. Lett. **94**, 093902 (2005).
127. S. Ghosh, A. R. Bhagwat, C. K. Renshaw, S. Goh, A. L. Gaeta, and B. J. Kirby, "Low-light-level optical interactions with rubidium vapor in a photonic band-gap fiber," Phys. Rev. Lett. **97**, 023603 (2006).
128. V. R. Almeida, Q. Xu, C. A. Barrios, M. Lipson, "Guiding and confining light in void nanostructure," Opt. Lett. **29**, 1209–1211 (2004).
129. J. T. Robinson, C. Manolatou, L. Chen, M. Lipson, "Ultrasmall mode volumes in dielectric optical microcavities," Phys. Rev. Lett. **95**, 143901 (2005).
130. G. S. Wiederhecker, C. M. B. Cordeiro, F. Couny, F. Benabid, S. A. Maier, J. C. Knight, C. H. B. Cruz, H. L. Fragnito, "Field enhancement within an optical fibre with a subwavelength air core," Nature Photonics **1**, 115–118 (2007).

1. Introduction

Nonlinear optical processes benefit from high optical intensities and long interaction lengths. In a bulk geometry, achieving higher intensities from a fixed optical power requires tighter focusing. However, such focusing leads to a shortened interaction length due to the reduced confocal parameter, which for many nonlinear processes results in no net increase in efficiency despite the higher intensities. Waveguiding geometries, such as optical fibers enable high optical intensities over extended interaction lengths as long as km's. However, dispersion and loss act to cap the effective interaction length for nonlinear processes, and further improvements in efficiency require increasing the material nonlinearity of the waveguide or increasing the effective nonlinearity by further reducing the guided-mode area. This pursuit of ever-smaller guided-mode areas spawns the question, how small can one make the waveguide core and still confine light?

Calculations show that the minimal dimensions are sub-micron for most high-index contrast structures [1–7]. Waveguides with sub-micron dimensions are known as photonic nanowires and are fabricated from a variety of materials, including silica glass [8–10], SF6 glass [11], chalcogenide glass [12], silicon [13, 14], InGaAs [15], and AlGaAs [16]. Examples of such waveguides are shown in Fig. 1. In addition to enhanced nonlinearities, ultra-small core waveguides provide other useful properties such as highly engineerable group-velocity dispersion (GVD) [5,6,17–20], reduced free-carrier lifetimes in semiconductors [21–23], and a minimal optical footprint for optimal integration of photonic chips. The combination of these properties enables impressive demonstrations of the applicability of maximally confining waveguides including all-optical modulators, switches, pulse delays, regenerators, amplifiers, pulse compressors, and wavelength converters.

#89450 - $15.00 USD Received 6 Nov 2007; revised 5 Jan 2008; accepted 5 Jan 2008; published 16 Jan 2008
(C) 2008 OSA

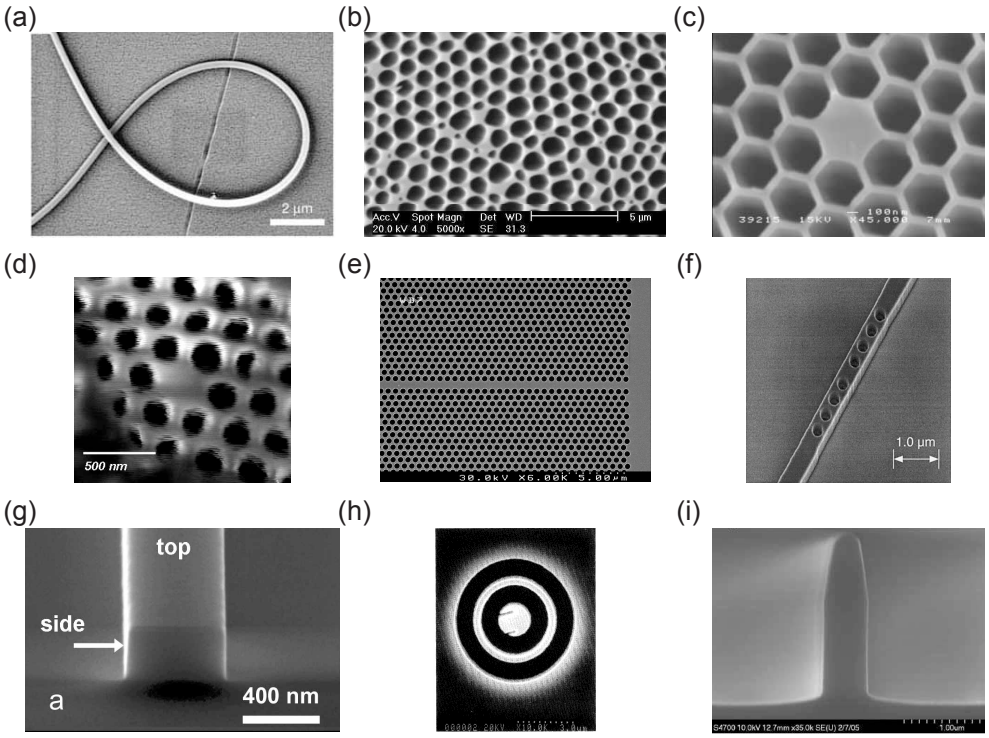

Fig. 1. Examples of various types of glass and semiconductor photonic nanowires. (a) Silica glass photonic nanowire [8]. (b) Cross-section of a random hole silica glass microstructured fiber in which the interstitial regions are used as sub- m guiding cores [9]. (c) Cross-sections of a tapered silica-glass microstructured fiber [10] and a (d) tapered SF6-glass microstructured fiber [11]. (e) Chalcogenide glass planar nanowaveguide with a microstructured photonic crystal cladding [12]. (f) Silicon nanowaveguide with an integrated resonant structure [13]. (g) Cross-section of a unclad silicon nanowaveguide [14]. (h) InGaAs photonic nanowire ring laser (top view) [15]. (i) Cross-section of an AlGaAs photonic nanowire [16].

2. Maximal nonlinearity

For large index contrast structures the dimensions of maximal confinement for the visible and near-infrared wavelength regimes are sub-micron. As an example, we consider two prototypical systems: a glass-rod-in air confining 800-nm light and a rectangular 1-to-1.5 aspect ratio embedded silicon-on-insulator waveguide confining 1550-nm light in the TE polarization mode. In Fig. 2 we plot the mode intensity profile for several different core areas. For core areas of 1 m^2, the mode stays well confined to the core for both materials. As the dimensions are reduced below 1 m, the mode area undergoes the same decrease. Eventually, as the waveguide dimensions are further reduced, the evanescent field begins to dominate, and the waveguide no longer tightly confines the light. This point is reached sooner in the glass-rod-in-air due to the lower index contrast. In this evanescent regime, the effective nonlinearity is diminished if the nonlinear material is assumed to be solely in the core. This confinement behavior determines the optimal size for the effective nonlinearity of the waveguide as illustrated in Fig. 3 [1–7].

The confinement behavior described above is universal to all index-guiding structures and many potential materials exist for nonlinear photonics. Although determining the precise dimensions for optimization requires modeling of the exact waveguide of interest, the following empirical relationship has been developed [5] and verified theoretically [24] to predict the op-

#89450 - $15.00 USD Received 6 Nov 2007; revised 5 Jan 2008; accepted 5 Jan 2008; published 16 Jan 2008
(C) 2008 OSA

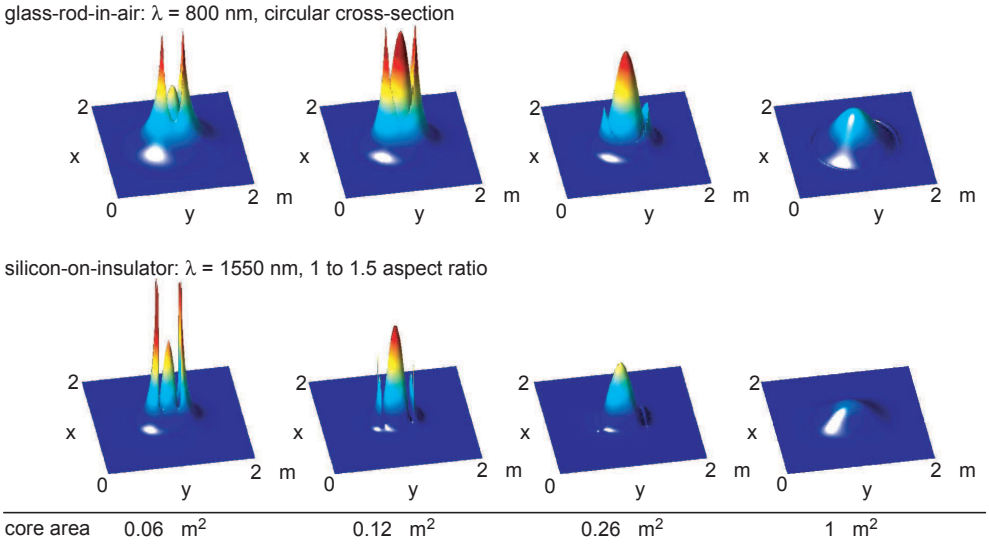

Fig. 2. Field intensity distribution inside glass-rod-in-air and silicon-on-insulator photonic nanowires for various sub-micron core sizes and wavelengths of 800 nm (glass-rod-in-air) and 1550 nm (silicon-on-insulator). The field remains confined as the core is reduced until a point at which the evanescent field dominates. This point occurs at larger core areas in the glass-rod-in-air due to the smaller index contrast.

timal core area as a function of wavelength and core and cladding indices of refraction:

$$\mathscr{A} = \frac{0.573\lambda^2}{(n_{core}+n_{clad})^{1.2}(n_{core}-n_{clad})^{0.8}}, \tag{1}$$

where $\mathscr{A}$ is the optimal core area, λ is the vacuum wavelength, n_{core} is the core index of refraction, and n_{clad} is the cladding index of refraction. Using this relationship, one can readily predict what dimensions are optimal for maximal confinement of propagating light in a wide variety of new materials. Since the optimal core area is relatively consistent among waveguides

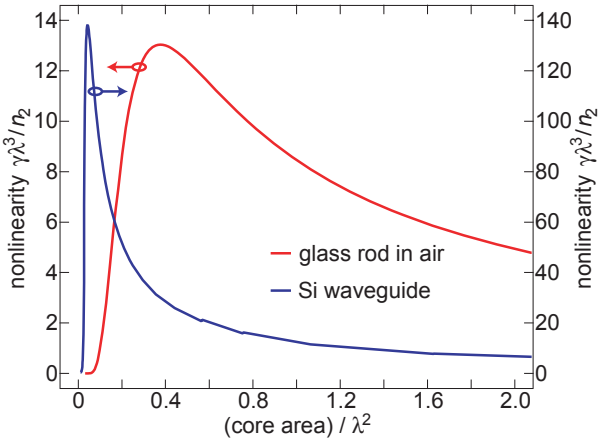

Fig. 3. Nonlinearity as a function of core area of a silica glass rod in air and silicon waveguide with a 1-to-1.5 aspect ratio embedded in a SiO_2 cladding.

#89450 - $15.00 USD Received 6 Nov 2007; revised 5 Jan 2008; accepted 5 Jan 2008; published 16 Jan 2008
(C) 2008 OSA

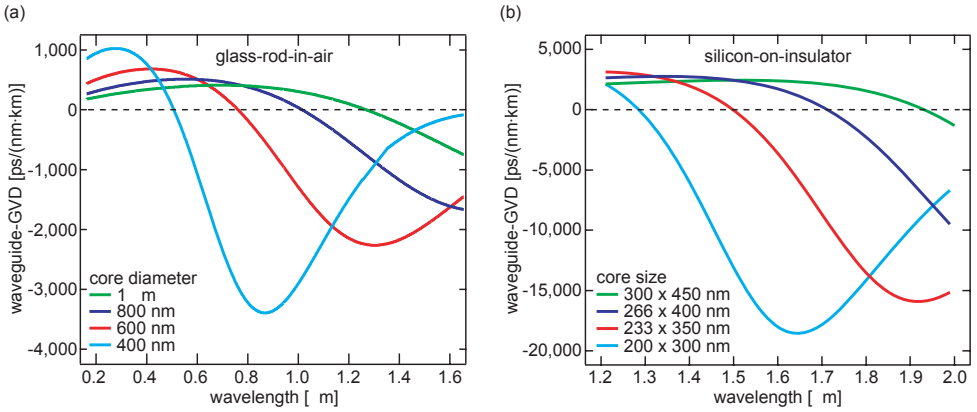

Fig. 4. Waveguide contribution to the group-velocity dispersion (GVD) in (a) silica-glass and (b) silicon photonic nanowires of various dimensions. As the core is reduced in size, the point at which the waveguide-GVD changes from anomalous to normal shifts to shorter wavelengths. The overall behavior of the waveguide dispersion among nanowires of different materials exhibits similar features that occur at smaller (larger) characteristic dimensions for larger (smaller) index contrasts.

of various rectangular and elliptical cross-sectional shapes this optimal area can be determined independent of the desired cross-sectional shape [5]. A rule of thumb is to use slightly larger than the optimal dimensions, since the nonlinearity falls off rapidly for waveguide dimensions smaller than optimal, as seen in Fig. 3.

Typically, other factors such as propagation loss and group-velocity dispersion will determine the precise waveguide dimensions. Nevertheless, due to the high sensitivity of confinement in photonic nanowires to wavelength and to waveguide dimensions, these parameters can be highly-controlled while remaining close to the optimal effective nonlinearity.

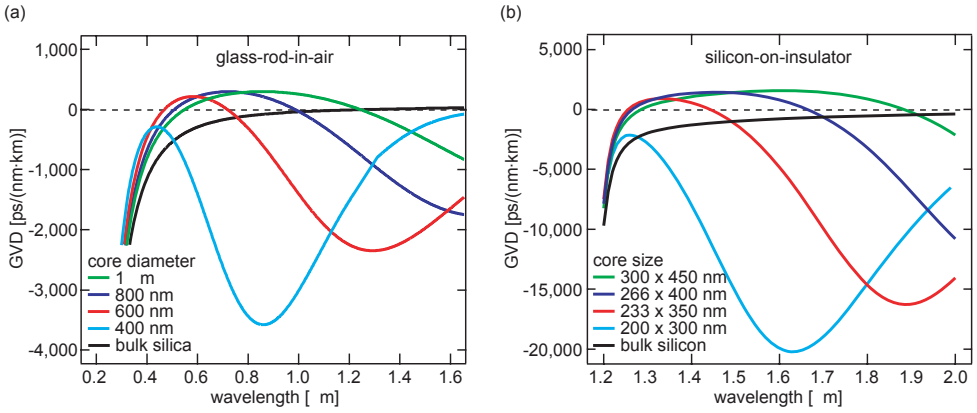

Fig. 5. Net group-velocity dispersion of (a) silica glass photonic nanowires and (b) silicon photonic nanowires of various dimensions compared to the bulk dispersion of their respective core material. As the core is reduced in size the zero-GVD points shift to shorter wavelengths. The overall behavior of the net-GVD is characterized primarily by the waveguide-GVD (Fig. 4) and is consistent among nanowires of different materials although they occur at smaller (larger) characteristic dimensions for larger (smaller) index contrasts.

#89450 - $15.00 USD Received 6 Nov 2007; revised 5 Jan 2008; accepted 5 Jan 2008; published 16 Jan 2008
(C) 2008 OSA

3. Engineered dispersion

For many nonlinear optical processes, the group-velocity dispersion (GVD) of a device is of critical importance [25]. The GVD controls the broadening of ultrafast pulses, the walkoff between pump and probe pulses, the phase-matching of parametric processes, and the generation of temporal optical solitons. The GVD in a waveguiding geometry is determined by both the intrinsic material dispersion and by a contribution from the confinement of the waveguide. For typical low-index contrast waveguides with core sizes on the order of a few microns, the GVD is characterized mainly by the material-GVD with a small correction due to the waveguide contribution [26, 27]. However for large index contrast waveguides, the waveguide dispersion plays an increased role, which allows for a high degree of GVD engineering and the high-impact demonstration of supercontinuum generation using 800-nm Ti:Sapphire pulses in several micron diameter silica microstructured fibers [28–34]. As the core is reduced to sub-micron dimensions in these high index contrast waveguides, the waveguide dispersion becomes dominant to the degree that in photonic nanowires the material dispersion is a small correction to the waveguide dispersion allowing the overall-GVD to be highly engineered [5, 6, 17–20].

The waveguide contribution to the GVD exhibits universal features among photonic nanowires of various materials. Figure 4 shows plots of the waveguide contribution to the GVD for (a) a glass-rod-in-air of various sub-micron dimensions and (b) a rectangular 1-to-1.5 aspect ratio embedded silicon-on-insulator waveguide of various dimensions. In both cases, as the core area is reduced, the first zero-GVD point is pushed to shorter wavelengths, and with further reduction in size, a second zero-GVD point is pushed into the near infrared until eventually a region of large normal-GVD reaches the wavelengths of interest. This behavior resulting from the waveguide dispersion is shared by all nanowires although for larger index contrasts the magnitude of the GVD increases and the shifts between anomalous-GVD and normal-GVD occur at smaller characteristic dimensions.

Figure 5 shows the net-GVD of the photonic nanowires when the material-GVD of the core is included. Comparison of Figs. 4 and 5 illustrates the dominance of the waveguide dispersion over the material dispersion for photonic nanowires. At the respective wavelengths of interest (800-nm and 1550-nm), a wide variety of net-GVD values are accessible. For the silica photonic nanowire GVD values from 300 to -3,500 ps/(nm·km) are achievable at 800-nm compared to the material GVD of -100 ps/(nm·km). In the silicon-on-insulator nanowaveguide, an even larger range of values of 1,500 to -18,200 ps/(nm·km) is achievable as a result of the large index contrast, despite the the larger material GVD of silicon of -900 ps/(nm·km). As photonic nanowires of new materials are developed, the same flexibility in the net-GVD can be expected due to this dominant contribution from waveguide dispersion.

4. Silica-glass photonic nanowires

Much of the interest in silica glass photonic nanowires began after a demonstration of fabrication and guiding in 100-nm scale glass fibers by Tong et al. [8] in 2003. This interest quickly lead to new methods for fabrication including flame and resistive heat tapering of single-mode fiber [10, 35–37], tapering of microstructured fiber such that the core diameter is sub- m in size [6, 10, 38, 39], and drawing photonic nanowires directly from bulk glass [40]. The use of tapered single-mode fiber provides nanowires with access to the evanescent field as well as a model glass-rod-in-air system while the tapering of microstructured fiber provides a more mechanically and environmentally robust structure since the outer diameter can remain much larger than 1 m. A hybrid technique has also been demonstrated in which using microstructured fiber one can taper small regions and gain access to the evanescent field [41]. These systems have found applications both in linear optics as sensors and in nonlinear optics for supercontinuum generation and other forms of frequency conversion. In this paper, we will focus

#89450 - $15.00 USD Received 6 Nov 2007; revised 5 Jan 2008; accepted 5 Jan 2008; published 16 Jan 2008
(C) 2008 OSA

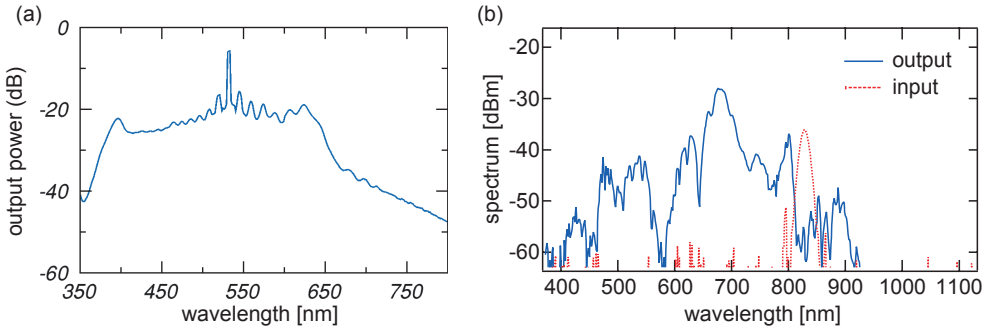

Fig. 6. Supercontinuum generated in silica glass photonic nanowires. (a) Generated spectra from a 2-cm long 510-nm diameter tapered single-mode fiber using 600-ps 140-nJ pulses with a 532 center wavelength [10]. (b) Generated spectra from a 3.5-cm long 650-nm diameter tapered microstructured fiber using 25-fs 125-pJ pulses with an 820-nm center wavelength [39].

on the nonlinear optical applications. In particular, photonic nanowires are used to lower the threshold for supercontinuum generation, allow for efficient pulse-compression approaching single-cycle durations, and allow for novel phase matching regimes for efficiently generating UV to visible dispersive radiation. Both the maximal nonlinearities and dispersion engineering available in photonic nanowires are crucial to the realization of these applications.

4.1. Supercontinuum generation

Nonlinear optical research in tapered and microstructured fibers has primarily focused on extreme spectral broadening of an injected light field [28–34]. For this reason the initial nonlinear optical experiments using silica-glass photonic nanowires were directed at making these processes more efficient as a result of the increased effective nonlinearity. Several experimental investigations have demonstrated low-threshold supercontinuum generation (SCG) in sub-micron core fibers for femtosecond [37,39] and nanosecond [10] pump pulses. In general, larger spectral broadening was observed in fibers with smaller core diameters for corresponding lengths and pump powers. Still, the maximal spectral extent achievable in photonic nanowires is reduced from that of larger core fibers due to the positioning of the anomalous-GVD regime on the short wavelength side of the pump. This positioning clamps the Raman self-frequency shifting of generated solitons to the nearby second zero-GVD point. Using photonic nanowires, octave-spanning white-light spectra are generated with kW peak pump powers and distances of less than 2 cm [10,39], as shown in Fig 6.

While these experiments highlight a general improvement in power requirements due to the larger effective nonlinearity, other factors including dispersion, wavelength-dependent loss, a wavelength-dependent nonlinearity, and multiple-stage spectral broadening typically contribute significantly to the resulting spectral extent and structure. The impact of these factors has lead to improved theoretical models that better match the observed spectra and distinguish the relative impact of these factors on the nonlinear propagation [42–44]. Specifically, inclusion of the wavelength-dependent nonlinearity is found to increase the predicted short-wavelength spectral extent of the continuum as compared to a model excluding this effect [43]. For larger fibers this effect was shown to modify the timescale of the self-steepening effect and for long wavelength pumps lead to a reduced Raman-self frequency shift and therefore a decreased long wavelength extent to the continuum spectrum [44]. Furthermore, the wavelength dependent loss was shown to cause a sharp long-wavelength cutoff and an asymmetry in the spectral extent of the contin-

#89450 - $15.00 USD Received 6 Nov 2007; revised 5 Jan 2008; accepted 5 Jan 2008; published 16 Jan 2008
(C) 2008 OSA

uum for small core diameters [45,46].

Rich propagation dynamics result from the multiple-stage continuum process in tapered microstructured fibers. In one experiment ultrashort pulses where launched in the anomalous-GVD regime near the first dispersion point of an untapered 2.3- m core diameter microstructured fiber. The self-phase modulation in the initially untapered fiber lead to the generation of several spectrally separated solitons. Once these solitons reach the sub- m tapered region, the solitonic conditions change due to the larger nonlinearity and the modified dispersion. This lead the initially generated solitons to each undergo further spectral broadening in the tapered region allowing for a greater extent of the supercontinuum particularly in the visible regime [45]. While this multiple-stage continuum was initially demonstrated using photonic nanowires, similar multiple-stage broadening processes have been shown to increase visible components of SCG in fibers with cores larger than 1- m [47–49].

4.2. Pulse compression

Beyond increasing the efficiency of nonlinear processes such as SCG, the use of photonic nanowires allows for propagation in novel dispersive regimes. Typically, for SCG the input pulse is launched in the anomalous-GVD regime and has a pulse energy corresponding to a higher-order soliton. The soliton order is given by $N = \sqrt{L_D/L_{NL}}$, where $L_D = {T_{in}}^2/|\beta_2|$ is the dispersion length, $L_{NL} = 1/(\gamma P_0)$ is the nonlinear length, T_{in} is the duration of the input pulse, β_2 is the GVD at the center wavelength, γ is the effective nonlinearity, and P_0 is the peak power of the input pulse. Launching a higher-order soliton allows the propagating pulse to undergo soliton-effect compression [25]. In the initial stages of SCG, the propagating pulse spectrally broadens and compresses slightly but then inevitably breaks apart into a series of solitonic components, which has been termed soliton fission [30]. The engineerable dispersion of photonic nanowires allows one to choose the dispersive conditions to maintain the phase overlap of the broadened spectrum during the initial stages of SCG and thus delay soliton fission. In this way, increased soliton-effect compression is possible. If the photonic nanowire is cut short enough that the pulse exits prior to fission, then a compressed pulse is available for further interactions and measurement [50].

To achieve broadband soliton effect compression, one requires a large region of anomalous-GVD with low third-order dispersion. The GVD engineering available with photonic nanowires allows for such optimization. Specifically, the use of silica photonic nanowires with diameters on the order of the wavelength of the guided light allows for such a dispersive regime. Futhermore for typical sub-100-fs input pulses, the photonic nanowire length must be on the order of a millimeter. Operating under these conditions, the propagating pulse is compressed efficiently to extremely short durations in the initial stages of spectral broadening and exits the waveguide before soliton fission. Compression of 70-fs pulses to 6.8 fs pulses has been experimentally demonstrated as shown in Fig 7 and simulations and preliminary measurements predict single-cycle pulse durations are possible [50,51]. While fibers with core diameters larger than 1- m also allow for considerable soliton-effect compression, compression factors as large as those achievable in photonic nanowires are not expected due to the increased third-order dispersion [52].

4.3. UV-visible dispersive-wave generation

Cherenkov radiation is associated with the generation of optical waves from particles traveling faster than the speed of light in a material. However, it can also be observed in radiation emitted from short pulses of light [30, 53, 54]. This effect has lead to some confusion since pulses of light certainly cannot travel faster than their own luminal velocity. The Cherenkov type phase-matching results from the definite phase relationship between the propagating pulse and

#89450 - $15.00 USD Received 6 Nov 2007; revised 5 Jan 2008; accepted 5 Jan 2008; published 16 Jan 2008
(C) 2008 OSA

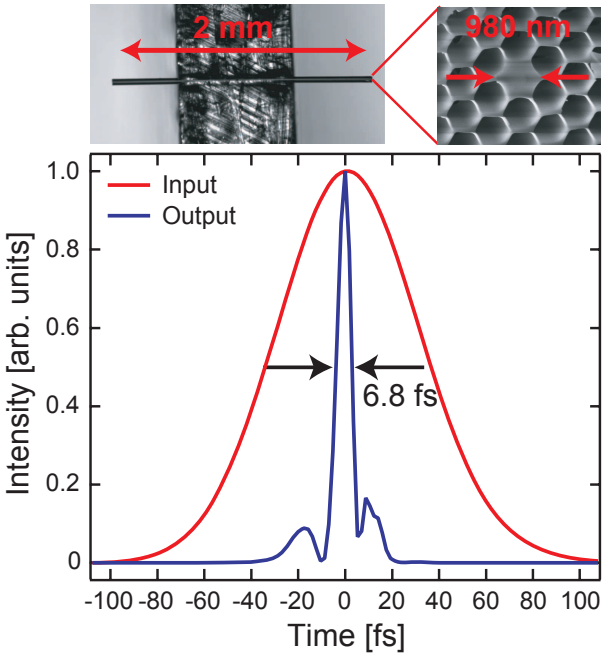

Fig. 7. Retrieved few-optical-cycle pulse self-compressed from the 70-fs input pulse by propagation in the 980-nm core diameter and 2-mm-long photonic nanowire pictured above the plot [50].

the emitted radiation, which does not exist for superluminal particles. This phase relationship allows the pulse to travel at its luminal group velocity but phase-match to dispersive waves in much the same way as the superluminal particle.

Consider a pulse of light traveling from point A to point B separated by a distance Δz. This pulse of light starts at point A at time $t = 0$ with a phase of $\phi_A = 0$. At point A the pulse generates a dispersive wave with a phase of $\phi_A = 0$. The pulse then travels to point B at its group velocity v_g and therefore arrives at point B at time $t = \Delta t = \Delta z/v_g$. In traveling to point B, the pulse accumulates a phase as a result of the distance traversed and the time expired. The phase of the pulse at point B is then $\phi_B = n(\omega_p)\omega_p \Delta z/c - \omega_p \Delta t + n_2 I \omega_p \Delta z/(2c)$, where n is the index of refraction, n_2 is the nonlinear index of refraction, ω_p is the angular frequency of the pulse, c is the speed of light, and I is the intensity of the pulse. If this pulse generates further dispersive radiation at point B and time $t = \Delta t$, this second dispersive wave will have an initial phase of ϕ_B. For the generated dispersive radiation to be phase matched, the phase accumulated by the dispersive wave traveling from point A to B in time Δt must be equal to the phase of the second emitted dispersive wave at point B and time $t = \Delta t$. This condition leads to the established phase matching condition of dispersive waves emitted by solitonic pulses [30], that is,

$$\frac{n(\omega_d)\omega_d}{c} - \frac{\omega_d}{v_g} = \frac{n(\omega_p)\omega_p}{c} - \frac{\omega_p}{v_g} + \frac{n_2 I \omega_p}{2c}. \tag{2}$$

While the ability to phase-match radiation is clear, the connection to Cherenkov radiation is not as obvious. The essential difference between a particle and the pulse is that the particle emits radiation with a constant initial phase. In contrast, the dispersive wave generated by the pulse is emitted with an initial phase that is directly related to the accumulated phase of the pulse as it propagates. Furthermore, the dispersive wave that is emitted at point B with an initial phase

#89450 - $15.00 USD Received 6 Nov 2007; revised 5 Jan 2008; accepted 5 Jan 2008; published 16 Jan 2008
(C) 2008 OSA

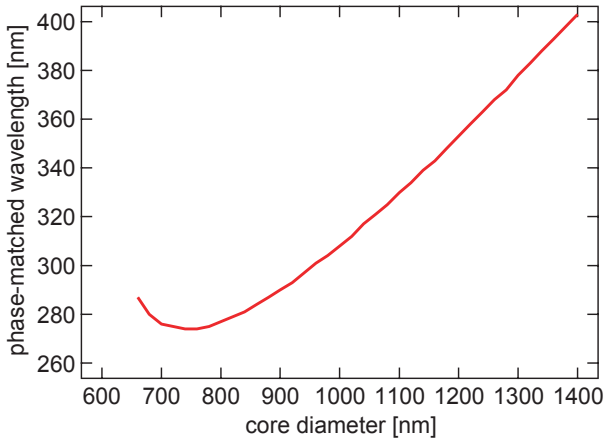

Fig. 8. Wavelength of phase-matched dispersive radiation as a function of core diameter of a silica-glass photonic nanowire.

is identical to a dispersive wave emitted at point B with zero phase at the same position but at an earlier time such that

$$\Delta t_{eff} = \frac{\Delta z}{v_g} - \frac{\omega_p \Delta z}{\omega_d c}\left[-n(\omega_p) + \frac{c}{v_g} - \frac{n_2 I}{2}\right]. \tag{3}$$

In this way, the pulse effectively arrives at point B at an earlier time Δt_{eff} and therefore is effectively the same as a particle traveling with a velocity given by

$$\frac{1}{v_{eff}} = \frac{\Delta t_{eff}}{\Delta z} = \frac{1}{v_g} - \frac{\omega_p}{\omega_d c}\left[-n(\omega_p) + \frac{c}{v_g} - \frac{n_2 I}{2}\right]. \tag{4}$$

The angle of generated Cherenkov radiation, θ is dependent on this effective velocity compared to the velocity of the dispersive radiation v_d by $\cos\theta = v_d/v_{eff}$. For a dispersive wave to build up in a waveguide geometry, this wave must be generated in the forward direction $\theta = 0$, that is, $v_{eff} = v_d = c/n(\omega_d)$. Applying this criteria leads to the condition

$$\frac{n(\omega_d)}{c} = \frac{1}{v_g} - \frac{\omega_p}{\omega_d c}\left[-n(\omega_p) + \frac{c}{v_g} - \frac{n_2 I}{2}\right] \tag{5}$$

which is identical to Eq. 3. Therefore, although the pulse travels at its luminal group velocity, it emits radiation with a phase equivalent to a superluminal particle traveling with the effective velocity given in Eq. 4. The definite phase relationship between the pulse and the generated dispersive wave, which does not exist for a typical charged particle, enables Cherenkov-type phase matching at subluminal group velocities.

While this phase-matching effect occurs for all solitons propagating in a material, its influence on SCG in nanowires is particularly pronounced. The GVD engineering available with photonic nanowires allows for a wide tunability to the phase-matched wavelength. In Fig. 8 we plot the wavelength of phase-matched dispersive waves versus the core diameter for a silica photonic nanowire and a pulse with an 800-nm center wavelength using Eq. 3 but neglecting the nonlinear term. As shown, the wavelength of the phase-matched dispersive wave decreases with the core diameter and then reaches a minimum for a sub-micron core diameter of 750 nm. Using this simple model to predict the phase matched wavelength indicates that photonic nanowires allow for the shortest wavelengths of dispersive waves to be generated during SCG.

#89450 - $15.00 USD Received 6 Nov 2007; revised 5 Jan 2008; accepted 5 Jan 2008; published 16 Jan 2008
(C) 2008 OSA

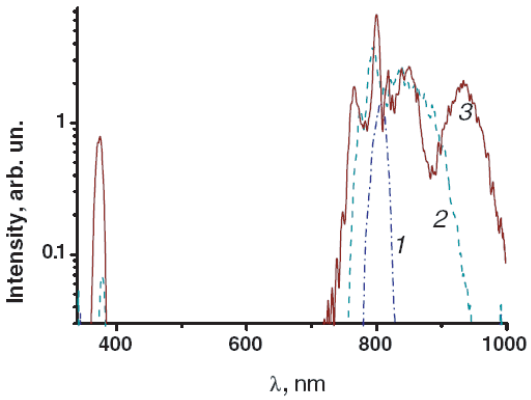

Fig. 9. Generation of 350-nm dispersive radiation using Cherenkov-type phase-matching in photonic nanowires [55].

Furthermore, decreased amplitude of the dispersive wave is expected for phase-matched wavelengths far from the pump due to the reduced overlap with the pulse spectrum. The wide bandwidth resulting from the efficient soliton-effect compression exhibited by photonic nanowires and discussed in the previous section further enhances the generation of this phase-matched radiation far from the pump leading the dispersive wave to be generated primarily during times of temporal compression [54]. Indeed light with wavelengths as short as 350 nm have been efficiently generated using photonic nanowires as shown in Fig. 9 [9,55]. This Cherenkov emission has been used to excite high-order modes of photonic nanowires [56] and as a mechanism for parametric amplification [57].

5. Silicon-on-insulator photonic nanowires

The larger index contrast of silicon-on-insulator (SOI) photonic nanowires allows for even tighter confinement of light. This enhancement combined with the larger Kerr nonlinearity of silicon allows for effective nonlinearities that are more than three orders of magnitude larger than those achievable in silica photonic nanowires, as shown in Fig. 3. In recent years, much work has focused on using this larger nonlinear response to create efficient nonlinear photonic devices. The highly developed fabrication and processing of silicon has aided in this pursuit. All optical devices based on two-photon absorption (TPA) [58–62], TPA-induced free-carrier dispersion [21,63–72], the Raman effect [22,73–81,83–87], and the Kerr effect [58,59,82,88–110] have all been demonstrated in silicon. Although extensive research in these areas has been carried out in waveguides with dimensions larger than a micron, in this review we will focus on the implementation of these processes in sub-micron waveguides or nanowaveguides. The bulk of research has focused on exploiting the large effective nonlinearity of these nanowaveguide structures and more recently, on the ability to engineer the GVD to optimize nonlinear processes which allows for new devices. Particularly for parametric processes, this GVD engineering has proven critical for optimal operation.

5.1. Two-photon absorption

Due to the band structure of silicon there exists efficient TPA at infrared wavelengths below 2.2 microns [58,59,111,112]. While the existence of TPA is often detrimental to nonlinear optical

#89450 - $15.00 USD Received 6 Nov 2007; revised 5 Jan 2008; accepted 5 Jan 2008; published 16 Jan 2008
(C) 2008 OSA

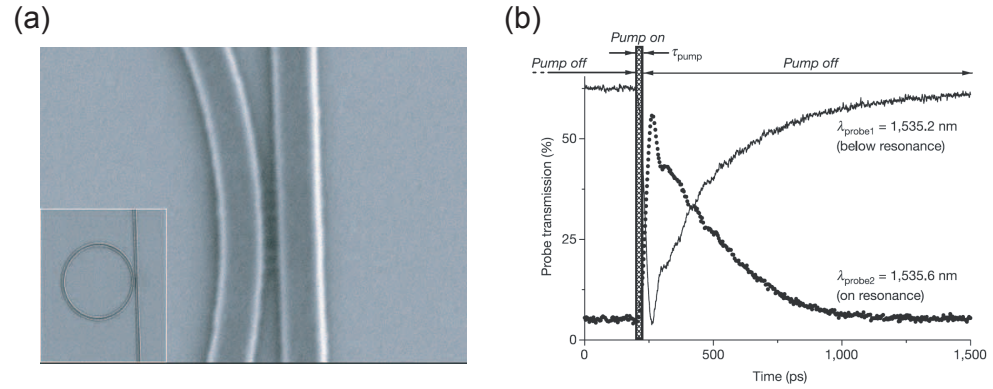

Fig. 10. An all-optical switch based on TPA-induced free-carrier dispersion in a silicon nanowaveguide ring resonator. (a) SEM image of the device. (b) Experimental switching realization [65].

processes, it has proven to be useful for a variety of photonic devices. Using solely TPA, an ultrafast switch has been demonstrated in silicon nanowaveguides requiring peak powers of 1.8 W for operation [61,62]. Furthermore, many all-optical devices using silicon nanowaveguides have made use of TPA-induced free-carrier injection. In this process, the photons absorbed through TPA generate free electrons and holes. The presence of these free carriers locally modifies the refractive index and the loss of the silicon structures such that [63],

$$\Delta n = -\frac{e^2\lambda^2}{8\pi^2 c^2 \varepsilon_0 n}\left[\frac{\Delta N_e}{m_{ce}^*} + \frac{\Delta N_h}{m_{ch}^*}\right], \tag{6}$$

$$\Delta\alpha = \frac{e^3\lambda^2}{4\pi^2 c^3 \varepsilon_0 n}\left[\frac{\Delta N_e}{m_{ce}^{*2}\ _e} + \frac{\Delta N_h}{m_{ch}^{*2}\ _h}\right], \tag{7}$$

where Δn and $\Delta\alpha$ are the changes in the index of refraction and absorption, respectively, e is the electronic charge, ε_0 is the permittivity of free space, n is the inherent refractive index of crystalline silicon, m_{ce}^* is the conductivity effective mass of electrons, m_{ch}^* is the conductivity effective mass of holes, $_e$ is the electron mobility, and $_h$ is the mobility of holes [63]. A major limitation of devices based on this effect is speed, and as such photonic nanowires provide an added advantage. The speed of devices based on carrier effects is generally limited by the free-carrier lifetime. For bulk silicon, the free-carrier lifetime is dependent on the level of doping. As the doping level is increased, the lifetime is reduced but is accompanied by an increase in optical loss. Using typical doping levels for optical purposes, the free-carrier lifetime of bulk silicon is on the s time scale. Therefore for silicon devices with large dimensions, the fastest devices based on free-carrier effects are limited to these speeds [64]. This lifetime can be reduced using a number of techniques including sweeping out carriers with a reversed-biased PIN structure [83] and ion implantation [113]. However, the simplest technique to reduce the carrier lifetime is to increase the rate of surface recombination. By making the waveguide cross-section smaller, the ratio of surface area to volume increases, and correspondingly the rate of surface recombination increases. Therefore using the smallest possible waveguide cross-sections (ie. photonic nanowires) provides the shortest free-carrier lifetimes and the fastest device performance with minimal added complexity.

Combining the extremely efficient TPA available in highly confining silicon nanowaveguides with the reduced free-carrier lifetimes available in nanowaveguides, optical bistability, all-optical switching, and all-optical wavelength conversion have been demonstrated in silicon

#89450 - $15.00 USD Received 6 Nov 2007; revised 5 Jan 2008; accepted 5 Jan 2008; published 16 Jan 2008
(C) 2008 OSA

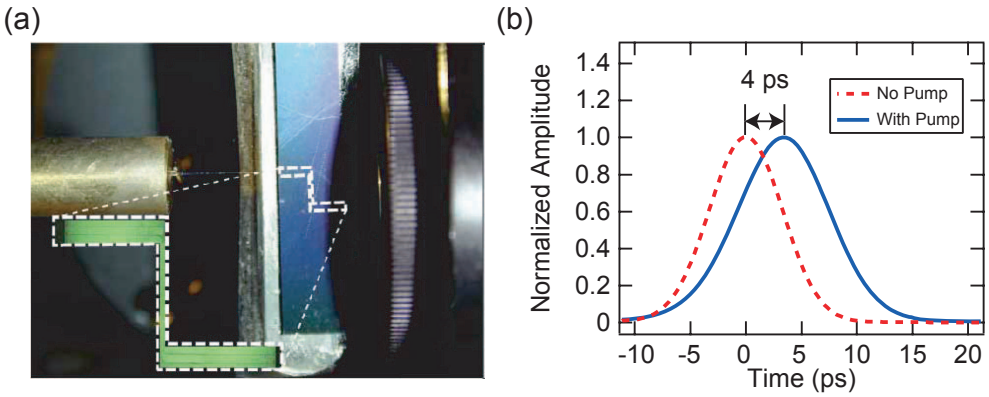

Fig. 11. All-optical pulse delay in a silicon nanowaveguide using stimulated Raman scattering. (a) Picture of the device. (b) Experimental measurement of a 1.3 pulse width delay [87].

nanowaveguides using power levels as low as 10 mW with free-carrier lifetimes of approximately 500 ps. [21,65,66,68–72]. As an example, an all-optical switch based on TPA-induced free-carrier dispersive tuning of an microresonator is shown in Fig. 10. By incorporating reverse-biased PIN structures, free-carrier lifetimes shorter than 50 ps have been reported for these nanowaveguide all-optical devices [67].

5.2. Raman amplification and oscillation

Silicon exhibits a strong and relatively narrow (∼1 nm) Raman response. Using this response, several Raman-based all-optical devices have been developed for the SOI platform. The achievement of large Raman amplification and Raman oscillation was demonstrated using large waveguide cross-sections and incorporating a PIN diode for CW operation [79,83–85]. A major hurdle to creating a Raman oscillator in silicon was the nonlinear loss resulting from TPA and TPA-induced free-carrier absorption (FCA). To remove FCA and to lower the power requirements for such devices, the use of silicon nanowaveguides can provide a benefit. As noted in the previous section, the use of photonic nanowires allows for a reduction in the free-carrier lifetime, which allows not only for faster devices but also reduces the build up of free carriers leading to lower densities and reduced losses incurred by FCA [76,77]. Using silicon photonic nanowires, Raman amplification of 3.1 dB without the need for a reversed-biased PIN structure has been demonstrated using peak pump powers of 2.8 W [22,78,80–82].

A further application of the efficient Raman process in silicon nanowaveguides has included slow light [86,87]. The narrow gain feature induced by the Raman effect creates a rapidly varying phase velocity as predicted by the Kramers-Kronig relations. This rapidly varying phase velocity leads to slow group velocities at the center of the gain feature. Utilizing this effect, all-optical delays of 1.3 pulse widths have been demonstrated in SOI photonic nanowires as shown in Fig. 11 [87].

5.3. Self-phase and cross-phase modulation

The tight confinement of SOI photonic nanowires allows for efficient effects derived from the Kerr nonlinearity. These parametric nonlinear processes often depend on the GVD for efficient operation. Perhaps the most straightforward parametric process to observe is that of self-phase modulation in which the Kerr-induced phase shift of a propagating pulse causes a red (blue) frequency shift on the front (back) of the pulse [25]. This effect generally characterizes the initial stages of supercontinuum generation discussed previously [34]. In silicon pho-

#89450 - $15.00 USD Received 6 Nov 2007; revised 5 Jan 2008; accepted 5 Jan 2008; published 16 Jan 2008
(C) 2008 OSA

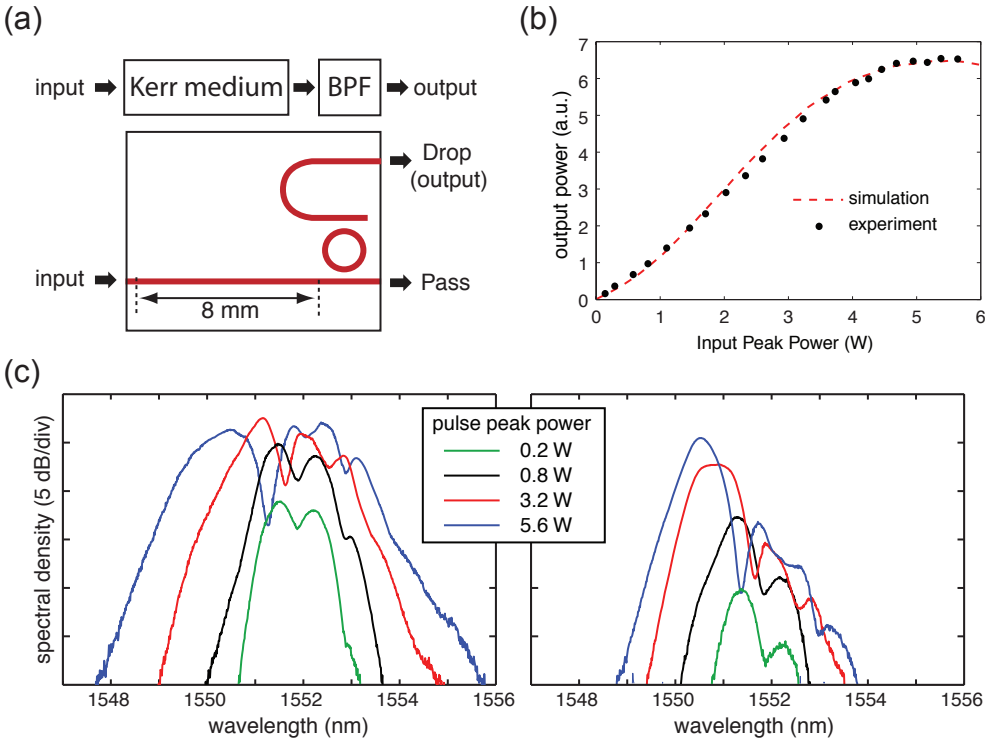

Fig. 12. All-optical SPM-based regenerator using a silicon nanowaveguide and integrated ring resonator band-pass filter (BPF). (a) Diagram of the device. (b) Experimental and simulated power transfer function. (c) Experimentally measured SPM broadening and filtered output for several pump powers [106].

tonic nanowires, self-phase modulation has been observed for both picosecond and femtosecond pulses [98,101]. Asymmetric spectral broadening is observed due to an additional rapid phase shift from the TPA-generated free-carriers, which aids the blue shift at the back of the pulse but opposes the red shift at the front. Additional spectral characteristics have been identified to result from dispersive-wave generation, from non-negligible third-order dispersion, and from soliton-formation [101,103,105,110].

With the incorporation of an integrated spectral filter, an all-optical regeneration device has been demonstrated [106] using silicon nanowaveguides based on the technique originally proposed by Mamyshev [114]. A schematic of the device is shown in Fig. 12(a). Signal regeneration relies upon a nonlinear power transfer through the device typically in the shape of an S-like step function, as shown in Fig. 12(b). This reduces the noise on the 0's and 1's of a data stream after being processed through the system. The silicon nanowaveguide device operates at 6-W peak powers, which represents an 8-fold reduction from previous integrated SPM-based techniques.

Cross-phase modulation is comparable to self-phase modulation except that the impact of the Kerr-induced phase shift occurs on a second generally weaker propagating pulse. Devices based on this effect have been demonstrated to be efficient in silicon photonic nanowires, and the effects of the GVD have been observed to greatly impact the interaction when the pulses are of significantly different wavelengths [99,104].

#89450 - $15.00 USD Received 6 Nov 2007; revised 5 Jan 2008; accepted 5 Jan 2008; published 16 Jan 2008
(C) 2008 OSA

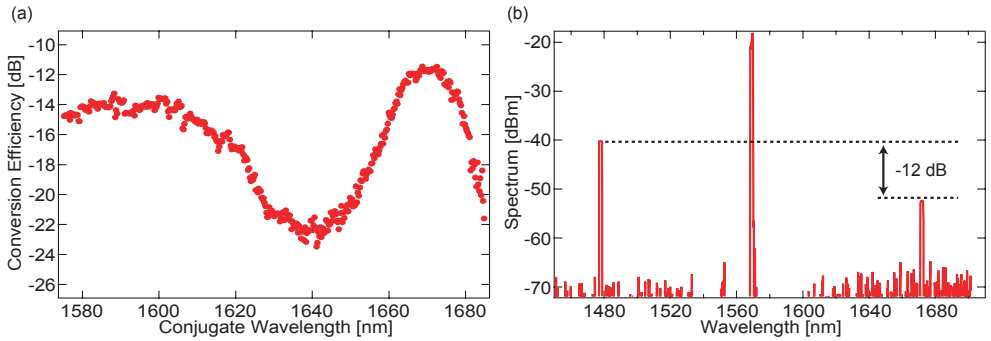

Fig. 13. Wavelength conversion across four telecommunications bands using four-wave mixing in silicon nanowaveguides (a) Conversion efficiency as a function of wavelength. The efficiency is shaped by the combined effects of the GVD and the fourth order dispersion of the nanowaveguide. (b) Experimentally observed FWM wavelength conversion from 1477 nm to 1672 nm [107].

5.4. Four-wave mixing

Four-wave mixing in silicon waveguides involves the third-order Kerr nonlinearity. This process has been shown to be efficient and broadband in silicon provided that the conditions of phase-matching are met [82, 88, 92–97, 100, 107]. Group-velocity dipsersion engineering of silicon photonic nanowires allows for the zero-GVD point or the anomalous-GVD region to be located in the C-band. In waveguides with near-zero-GVD, conversion of continuous-wave light can be achieved at efficiencies of -10 dB over bandwidths larger than 150 nm [97, 107]. Utilizing higher-order dispersion to achieve phase-matching wavelength conversion across four telecommunications bands has been achieved as seen in Fig. 13. In silicon nanowaveguides FWM wavelength conversion requires peak powers of only 100-mW. Furthermore, in a pulsed experiment and with waveguides exhibiting anomalous-GVD, it was demonstrated that parametric amplification is achievable with reduced free-carrier lifetimes using peak powers on the order of 1 W [95]. This demonstration indicates the potential for a wavelength-agile CMOS-compatible source on chip in the form of a FWM-based optical parametric oscillator.

Resonant enhancement of FWM has been demonstrated in silicon nanowaveguide ring resonators [109]. The addition of a resonant structure further reduces the peak power required to observe this nonlinear process. Using input peak powers below 1 mW, FWM wavelength conversion has been observed in a micrometer-scale silicon nanowaveguide ring resonator. The ability to observe nonlinear interactions at sub-mW power levels in a micrometer-scale device demonstrates the potential scalability of nonlinear optical devices on a single photonic chip. At these ultra-low power levels and sizes, it is possible to realize hundreds of devices operating simultaneously on a single chip.

Regeneration devices based on FWM have also been demonstrated in silicon photonic nanowires [108]. These processes rely on the ultrafast response of the FWM process and on the quadratic dependence on the pump power. Using a variety of pump and signal configurations, reshaping and retiming of actual 10-Gbps return-to-zero and non-return-to-zero data streams have been demonstrated using average powers of only 30 mW [108].

6. Future directions

As highlighted in the previous sections, extensive research has been carried out on applying maximally confining waveguides for nonlinear optical functionality. Nevertheless, many avenues remain unexplored. The majority of research has investigated nonlinear processes in sil-

#89450 - $15.00 USD Received 6 Nov 2007; revised 5 Jan 2008; accepted 5 Jan 2008; published 16 Jan 2008
(C) 2008 OSA

ica glass and silicon nanowaveguides, which is driven by the mature fabrication and broad availability of these materials. Other materials may have more favorable nonlinear properties such as $\chi^{(2)}$ responses, a larger $\chi^{(3)}$ response, or lower linear and nonlinear losses. Research into the nonlinear optical properties of photonic nanowires of these materials will undoubtedly emerge once the challenges of fabrication are overcome. Furthermore, many materials cannot be formed into waveguides. Photonic nanowires have potentially large evanaescent fields as seen in the 0.06 m^2 waveguides in Fig. 2. Using the access to the evanescent field available in photonic nanowires, integration of new materials, such as gases, with highly confining waveguides is emerging [115]. With these new areas of research, in addition to further applications of silica glass and silicon waveguides, photonic nanowires will continue to provide lower power levels and new functionalities to nonlinear optical devices.

6.1. Other materials

Research has begun on the fabrication and application of photonic nanowires from novel glasses with large nonlinear responses including SF6 and chalcogenides [11,116]. In particular chalcogenide glasses have a nonlinear response which is 2 to 3 orders of magnitude larger than silica glass and a relatively high linear refractive index. The combination of these two properties allows the effective nonlinearity of chalcogenide glass photonic nanowires to be more than 3 orders of magnitude larger than silica glass nanowires, which promises the extension of many applications of nonlinear optics in optical fibers to more readily achievable power levels. Self-phase modulation has been observed in tapered fibers of SF6 and chalcogenide glasses using peak power levels as low as 1 W. Core diameters as small as 400 nm have been achieved in SF6 glass, but nonlinear effects in sub-micron chalcogenide fibers have yet to be reported. Additionally, dispersion engineering and phase-matching of parametric processes such as FWM have not been experimentally demonstrated in photonic nanowires of these materials but should be expected in the near future with improved fabrication [116,117].

Other semiconductor materials are also being explored for implementation in nonlinear optical devices. Nanowaveguides have been fabricated from AlGaAs and GaAs and several demonstrations of efficient nonlinear processes such as self-phase modulation and FWM have been observed [16,118–121]. The linear propagation loss of these waveguides has typically impeded their performance, but with further improvements in the fabrication process this challenge will certainly be overcome. Dispersion engineering and anomalous-GVD near 1550 nm have recently been demonstrated in AlGaAs nanowaveguides [122]. Efficient nonlinear optics using III-V nanowaveguides promises new realms of integrated nonlinear optical devices incorporated with optically active III-V devices such as lasers, amplifiers, and modulators.

6.2. Evanescent nonlinearities

A wide variety of useful nonlinear optical materials intrinsically cannot be fabricated as waveguides such as gases and liquids. Through the potentially large evanescent fields, photonic nanowires provide a route towards incorporating these materials in a high-confinement guided-wave geometry. When the dimensions of a photonic nanowire are reduced slightly below the optimal confinement point, a large evanescent field is produced, as seen in Fig. 2. For a range of sizes, this mostly evanescent mode still has a relatively small mode-field area and thus a large effective nonlinearity. In Fig. 14 the effective nonlinearity for a silica photonic nanowire surrounded by an evanescent nonlinear material with an index close to 1 (i.e. a gas) is plotted as a function of core diameter for a wavelength of 800 nm. The optimal core diameter for evanescent nonlinearities is 340 nm. At this optimal size, the effective nonlinearity is more than an order of magnitude larger than those currently available in hollow-core photonic bandgap fibers, which is also a promising system for guided-wave integration with nonlinear

#89450 - $15.00 USD Received 6 Nov 2007; revised 5 Jan 2008; accepted 5 Jan 2008; published 16 Jan 2008
(C) 2008 OSA

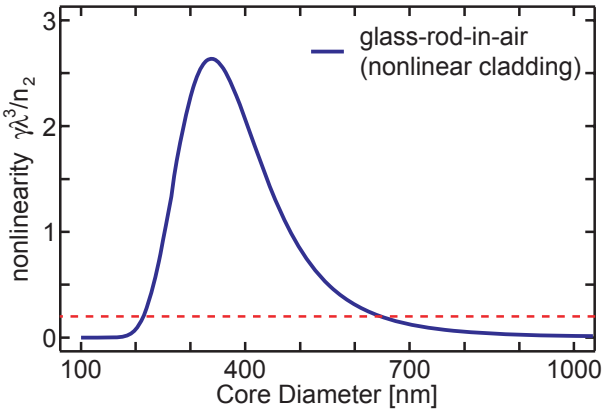

Fig. 14. Effective nonlinearity as a function of core diameter of a silica-glass photonic nanowire assuming a gaseous nonlinear cladding material with a nonlinear index coefficient n_2. As a comparison the effective nonlinearity of a commercially available 800-nm hollow-core photonic bandgap fiber (Crystal Fiber HC-800-02) with a 5- m mode field diameter and $\gamma\lambda^3/n_2 = 0.205$ is shown by the red dashed line.

gases [123–127]. Interactions with gases have been experimentally demonstrated using silica glass photonic nanowires [115], and integrated optical nanowaveguides have also been analyzed for this purpose with novel slot and hole geometries being explored to maximize the evanescent field strength [7, 128–130].

7. Conclusions

Photonic nanowires allow for maximal effective nonlinearities and a large degree of dispersion engineering. These properties in combination with the potentially large evanescent fields and minimal optical footprint allow such nanowaveguides to be ideally suited for a host of nonlinear optical interactions and devices. With the incorporation of new materials and the demonstration of novel effects, photonic nanowires should continue to provide unique nonlinear optical functionality at even lower power levels.

Acknowledgements

This work is funded by the Center for Nanoscale Systems, supported by the NSF and the New York State Office of Science, Technology and Academic Research, and the DARPA DSO Slow-Light Program.

#89450 - $15.00 USD Received 6 Nov 2007; revised 5 Jan 2008; accepted 5 Jan 2008; published 16 Jan 2008
(C) 2008 OSA